ISSN (e): 2250 – 3005 || Volume, 07 || Issue, 04|| April – 2017 ||
International Journal of Computational Engineering Research (IJCER)

Drag Optimization of Bluff Bodies using CFD for Aerodynamic Applications

Veeralkumar Thakur[1], Tarun Yadav[2], Dr. Rajiv B.[3]
[1]B. Tech, Production Engineering, College of Engineering, Pune, India,
[2]Manager, Hindustan Aeronautics Limited, Nashik, India,
[3]HOD, Production Engineering, College of Engineering, Pune, India

ABSTRACT
This paper deals with the optimization of bluff bodies and analysis of fluid flow behaviour around bodies using CFD. Three test cases of bluff bodies; mainly two-dimensional rectangular body, radial rectangular shape and bullet shaped body were considered in this paper. Their shapes were optimised to achieve aerodynamic body shape using drag coefficient as main criteria. The other aerodynamic characteristics like formation of different eddy loops due to eddy viscosity, lift force coefficient and pressure force with Mach number were also investigated. It is concluded that aerodynamically; bullet shaped body is best among all the cases.
Keywords:Aerodynamics, Bluff body, Computational Fluid Dynamics (CFD), Drag coefficient, Eddy viscosity, Mach number, Optimization

Nomenclature:
u = velocity
ρ= density
p = pressure
σ= shear stress
μ= dynamic viscosity
f= force
Re= Reynolds number
x,y,z = Cartesian co-ordinates
Sub-script:
i, **j**, **z** = directions in x, y, z respectively

I. INTRODUCTION

Bodies with attribute of a non-aerodynamic rectangular cross sections which have length of the body in the flow direction close or equal to that perpendicular to the flow direction are termed as bluff bodies. These bodies significantly disturb the flow around them, as opposed to flow around a streamlined body. Even a streamlined body such as an air-foil, passing through a fluid, behaves much like a bluff body at large angles of incidence. Bluff body flows are characterized by flow separation which produces a region of disturbed flow behind, which know as a wake region. A bluff body moving through a fluid experiences a drag force of two types: frictional drag, and pressure drag. Frictional drag comes from friction between the fluid flowing over the surface which is related to the development of boundary layers and the Reynolds number has a significant effect on it. Eddying motions give the rise to pressure drag that are generally formed in the fluid flow pattern by the body passing through it. Both types of drag are due to viscosity, but the distinction is made by the flow pattern generated by the two types of drag. Frictional drag is for attached fluid flows over a body with its surface area exposed to the flow. Pressure drag is important for separated flows, and it is related to the cross-sectional area of the body. Typical for bluff bodies, the principal contribution to drag experienced is pressure drag.The structure of a bluff-body fluid flow consists of three regions: the boundary layer along the bluff-body, the separated free shear layer, and the wake. At the leading edge of bluff body a boundary layer is formed and is finalized with the flow separation at its base. At the base, shear layers are initiated in the points of flow separation and recirculation bubble behind the bluff-body is organised when both the top and bottom layers are merged with each other and begin to combine. This phenomenon starts to form the wake. When Reynolds numbers, R_e<200000, with a length scale equal to the obstacle base, the boundary layer may be assumed as laminar. The forces exerted by the fluid stream over the body immersed in the flow stream, produces the normal and tangential stresses over the body's surface. After integration of these forces, these stresses give rise to the resultant load components, which are expressed in non-dimensional form, defined as follows:

$C_{F_i} = \frac{F_i}{1/2\rho U^2 S}$ ……….... (eq. 1.1)

$C_{M_i} = \frac{M_i}{1/2\rho U^2 S l}$ ……….... (eq. 1.2)

F_i is the force component and M_i is the moment acting on the body in the $x_i$direction of the resultant force.
U is the undisturbed upstream flow velocity
S is a reference surface
l is a reference length.
In optimization of bluff bodies, it is essential to understand thoroughly the behaviour of fluid flow around the bodies; this assists in designing with regard to the parameters such as principal features: shape of the body affecting aerodynamic drag. Principle feature influences the drag coefficient of 2D models of three different bluff bodies considered in this paper. This being the main objective, optimisation of body aerodynamics i.e. bluff body shape and its drag coefficient was achieved using numerical method of CFD for accurate numerical predictions of the different bluff-body flows. Fluid flow is defined by means of various characteristics like pressure and viscous forces, drag coefficient, eddy loops (i.e. vortex formations).

CFD is a tool which calculates numerical solutionsand enable us to predict quantities like aerodynamic drag, heat transfer, mass transfer, chemical reactions, and other relevant phenomena by solving the mathematical equations which are governed by the steady or unsteady, compressible and incompressible Navier-Stokes equations, including multi-species and finite-rate chemistry modelling.

II. LITERATURE REVIEW:

In the recent research in these areas, Sibha Veerendra Singh et al.[7] studied the flow behaviour of a nose cone bluff bodies of missiles and effects of pressure were validated by using results from calculations which shows from the fluent simulation that at high Mach number a detached bow shock at the front of the body generates, which highly influence the flow properties around the body and aerodynamic drag body initially depends on its kinetic energy and bluntness of the nose cone decrease the aerodynamic drag over the body by generating the strong bow shock. Whereas, research by Gera. B et al. [5] states the numerical simulation carried out for 2D unsteady flow pattern around a square cylinder to obtain the wake behaviour has been validated numerically for the Reynolds's number (Re). The study also predicted the influence of Re on quantities such as Strouhal number and lift, drag, and base suction coefficients. The lift coefficient and velocity component in the wake region were monitored for calculation of Strouhal number and the variation of Strouhal number with Reynolds number was found from the analysis.
The study conducted by Stefano Malavasi et al. [10] a numerical procedure for the simulation of the dynamic loading on a rectangular cylinder placed in a stationary flow has been validated and used to study the effect of an asymmetrical confined flow on the same cylinder. Phenomenon which is characterized by the presence of a high distortion of the vortex formations around the cylinder. Comprehensive study of the flow pattern generated around a rectangular cylinder at Reynolds number of 21400 with the influence of various simulation factors like mesh type, turbulence model etc., were validated by use of Reynolds averaged Navier-Stokes (RANS) models and large eddy simulation (LES). Drag coefficient, RMS value of lift coefficient, Strouhal number etc. Different instantaneous and time and span waise-average velocity, vortices magnitude was presented by Xuyong Ying et al.[2].In the report by G. Buresti et al. [8] possible methods for the reduction of the drag of heavy road-vehicles was the objective and activity of critical analysis of the gap flow in the basic different configurations used to simulate is in order to identify the effects of variation of the shape, position and dimensions of the slots, the direction of the flow.

III. NUMERICAL DESIGN AND MODELING:

The optimization of the bluff body was mainly associated with the principle feature i.e. the shape of the body. So, firstly 2D designs of three different bluff bodies was created with specified dimensions keeping the length and width of the body constant (*see Table 1.*) and optimizing other dimensions to obtain more aerodynamic shape i.e. the frontal area of contact with the fluid. Modeling is done ANSYS ICEM. Process of optimizing the bluff body is by changing its dimensions from a blunt surface towards more aerodynamic form. Primarily, 2D rectangular surface was designed and was further optimized to 2D radial geometry and lastly to attain the shape of the bullet. In this paper 'Aero-foil' was considered as the ideal aerodynamic shape *(see figures 1, 2, 3)*.
A 71mm x 12mm 2D rectangular design was chosen with the aim of full frontal contact of the body with the fluid resulting in maximum opposition and drag. Further improvement in rectangle shape was done by assigning a radial front area to the rectangular shape. Finally optimizing the shape, a bullet like shape was designed with specified dimensions (*see Table 1.*) to attain a more aerodynamic shape.

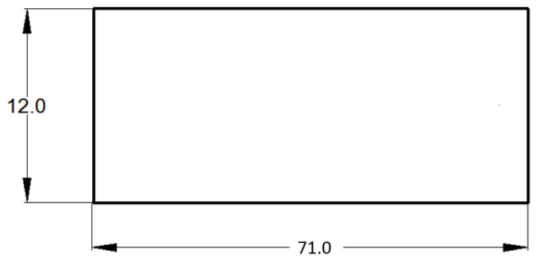

Figure 1. 2D geometry of rectangular bluff body

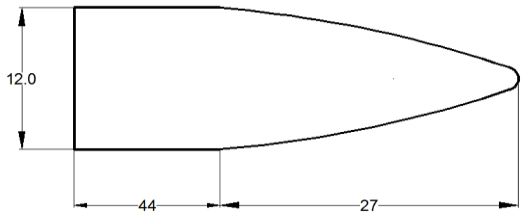

Figure 2. 2D geometry of radial rectangle bluff body

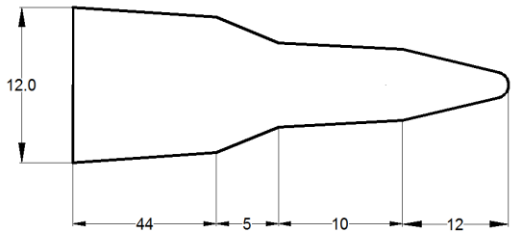

Figure 3. 2D geometry of bullet shaped bluff body

Sr. No	Body Shape	Length (mm)	Width (mm)	Frontal contact with fluid
1.	Rectangle	71	12	100%
2.	Radial-rectangle	71	12	80.98%
3.	Bullet Shaped	71	12	73.94%

Table 1. Dimensional Data

IV. CFD ANALYSIS AND SIMULATION:

The Using ANSYS products like ICEM and Fluent for meshing and CFD analysis, emphasis on carefully constructing the mesh grid, initialization and boundary conditions was considered.

4.1Mesh and Grid Generation:

The fine shell meshing for all three type of bluff bodies were generated in ICEM CFD software. A structured grid was generated by blocking method as seen in figure 7 & 8 for all the bluff body designs. All meshes are generated with quad elements using quad dominant mesh type.Table.2 shows the details of various grids.Figures4, 5, and 6 shows the wire frame of shell mesh patternof rectangular, radial-rectangular and bullet shaped respectively. The grids were sufficiently fine near the walls, away from the wall and boundaries to capture the exact fluid flow physics. After meshing, initialization and boundary conditions were set and CFD simulations in ANSYS-Fluent were carried out on all grids to analyze the fluid flow behavior of these bodies. The dimensional units in Fluent were set to SI.

4.2Discretization and Control Setup:

The pressure based solver with Spalart- Allmaras equation for viscous model was considered for simulations. In Solution controls, the Turbulence Viscosity were set to 0.8. The under-relaxation factors, only flow variables were considered as 0.25. In solution methods, the 2nd order upwind spatial discretizationwith Green-Gauss Node based gradient was set.

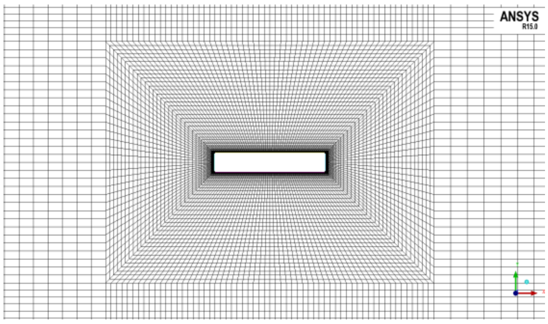

Figure 4. Mesh pattern for rectangle bluff body

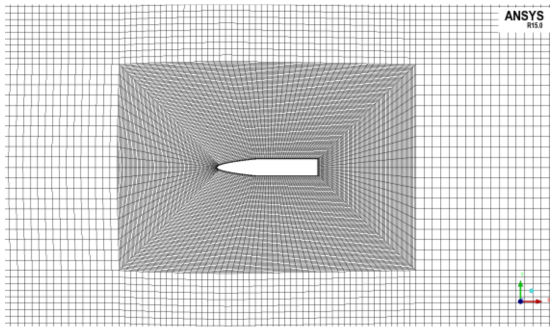

Figure 5. Mesh pattern for radial rectangular bluff body

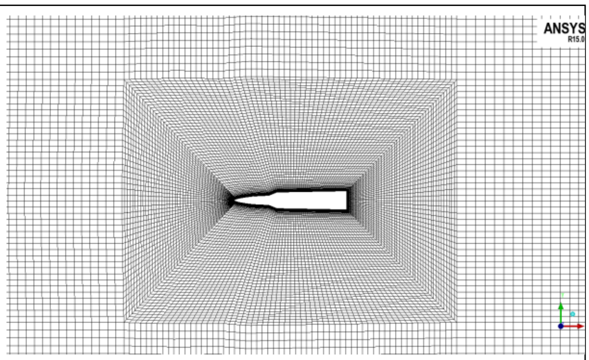

Figure 6. Mesh pattern for bullet shaped bluff body

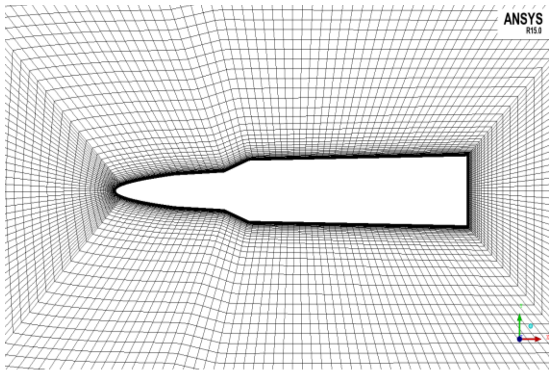

Figure 7. Structured mesh for bluff body

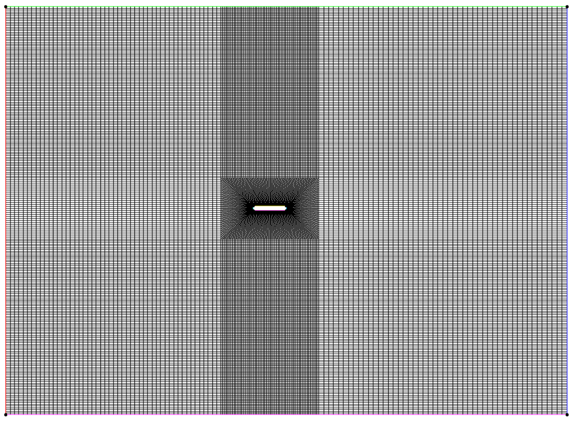

Figure 8. Grid pattern used for simulation

Sr. No.	Body Shape	Grid type	Number of Elements	Number of Nodes
1	Rectangular	Fine	50364	49880
2	Radial Rectangular	Fine	59046	58520
3	Bullet	Fine	67526	66960

Table 2. Grid Details

V. GOVERNING EQUATIONS:

Continuity equation:

$$\frac{\partial \rho}{\partial t} + \frac{\partial}{\partial x}\rho u_x + \frac{\partial}{\partial y}\rho u_y + \frac{\partial}{\partial z}\rho u_z = 0 \qquad \text{……… (eq. 6.1)}$$

Equation of motion:

Where ρ and μ are constants,

$$\rho\left(\frac{\partial u_x}{\partial t}+u_x\frac{\partial u_x}{\partial x}+u_y\frac{\partial u_x}{\partial y}+u_z\frac{\partial u_x}{\partial z}\right)=-\frac{\partial p}{\partial x}+\mu\left[\frac{\partial^2 u_x}{\partial x^2}+\frac{\partial^2 u_x}{\partial y^2}+\frac{\partial^2 u_x}{\partial z^2}\right]+\rho g_x$$

...…. (eq. 6.2)

$$\rho\left(\frac{\partial u_y}{\partial t}+u_x\frac{\partial u_y}{\partial x}+u_y\frac{\partial u_y}{\partial y}+u_z\frac{\partial u_y}{\partial z}\right)=-\frac{\partial p}{\partial y}+\mu\left[\frac{\partial^2 u_y}{\partial x^2}+\frac{\partial^2 u_y}{\partial y^2}+\frac{\partial^2 u_y}{\partial z^2}\right]+\rho g_y$$

…... (eq. 6.3)

$$\rho\left(\frac{\partial u_z}{\partial t}+u_x\frac{\partial u_z}{\partial x}+u_y\frac{\partial u_z}{\partial y}+u_z\frac{\partial u_z}{\partial z}\right)=-\frac{\partial p}{\partial z}+\mu\left[\frac{\partial^2 u_z}{\partial x^2}+\frac{\partial^2 u_z}{\partial y^2}+\frac{\partial^2 u_z}{\partial z^2}\right]+\rho g_z$$

…....... (eq. 6.4)

The core basic equations used for fluid simulation by CFD are Navier-Stokes equations which is given by,

$$\rho\left[\frac{du}{dt}+u\nabla u\right]=\nabla\sigma+f$$

………(eq.6.5)

$\rho$is equivalent to mass, $\left[\frac{du}{dt}+u\nabla u\right]$ is the acceleration,
$\nabla\sigma+f$represents the total force, in which the$f$ being all other forces acting on the body.
Other form of Navier-Stokes equation is given by,

$$\rho\frac{du}{dt}=-\nabla p+\mu\nabla^2 u+f$$

………. (eq. 6.6)

Here ∇^2 is the Laplacian operator
These equations are a set of nonlinear partial differential equations (PDEs) with assigned boundary conditions. The continuity equation and the general form of the Navier-Stokes equations, in tensor notation are,

$$\frac{\partial\rho}{\partial t}+\frac{\partial(\rho u_i)}{\partial x_i}=0$$

………(eq.6.7)

$$\frac{\partial(\rho u_i)}{\partial t}+\frac{\partial(\rho u_i u_j)}{\partial x_i}=-\frac{\partial\rho}{\partial x_i}+\frac{\partial}{\partial x_i}\left[\mu\left(\frac{\partial u_i}{\partial x_j}+\frac{\partial u_j}{\partial x_i}\right)\right]+F$$

………. (eq. 6.8)

The *eq. 6.7 and eq. 6.8* is the instantaneous acceleration term and the convection term respectively. It consists ofthe pressure gradient term plus the viscous dissipation term. In case of incompressible flowsρconstant.

VI. CFD RESULTS

The results of optimization of three different bluff body designs, each was optimized than the previous design. Throughout the simulation airflow was kept steady and incompressible. All parameters like pressure, density, velocity and temperature considered to be independent of time.

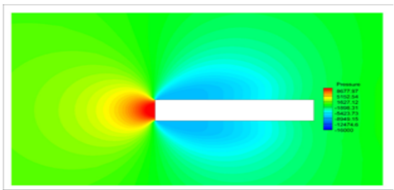

Figure 9. Pressure variation of rectangular bluff body

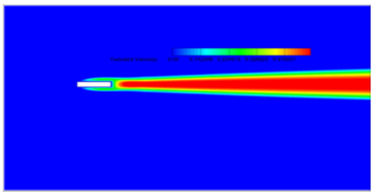

Figure 10. Turbulent viscosity of rectangular bluff body

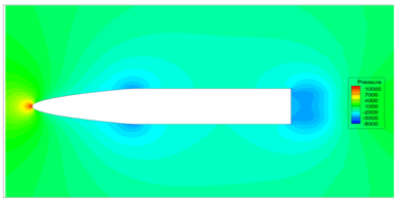

Figure 11. Pressure variation in radial rectangular bluff body

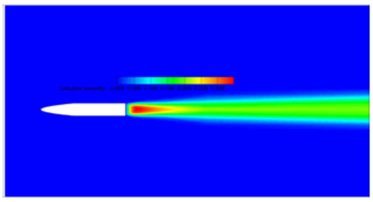

Figure 12. Turbulent viscosity variation in radial rectangular bluff body

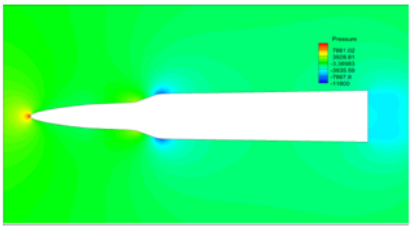

Figure 13. Pressure variation in bullet shaped bluff body

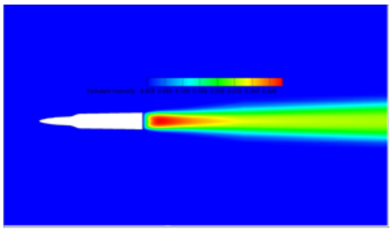

Figure 14. Turbulent viscosity variation in bullet shaped bluff body

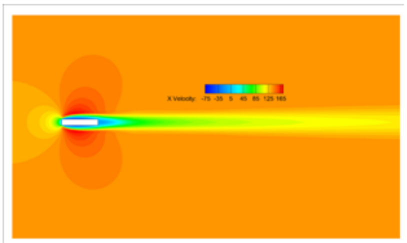

Figure 15. X-velocity variation in rectangular bluff body

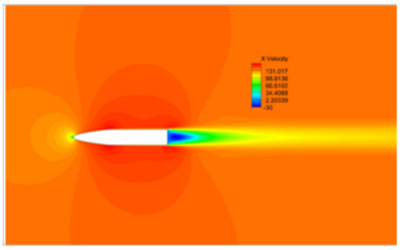

Figure 16. X-velocity variation of radial rectangular bluff body

Fig. 9, 11 and 13 shows the pressure variation around the bluff body design of rectangular shape, radial rectangular shape and bullet shape respectively. In rectangular shape as the frontal contact area is large, the maximum pressure at the front area and it drops around the walls due large eddy loop formation. In case of radial-rectangular shape and bullet shape body, the maximum pressure is near the radial tip of the body and the pressure drops are decreasing on the sides compared to the rectangular shape and shows optimization of the body towards the ideal aero foil shape. *Fig. 10, 12 and 14* shows the turbulent viscosity variation over the surface of the bluff bodies. Variation in the x-directional velocities of the bluff bodies are shown in *fig. 15, 16 and 17*. This gives the information of the velocities of the fluid at the different sections of the body travelling in x-y plane around the body.

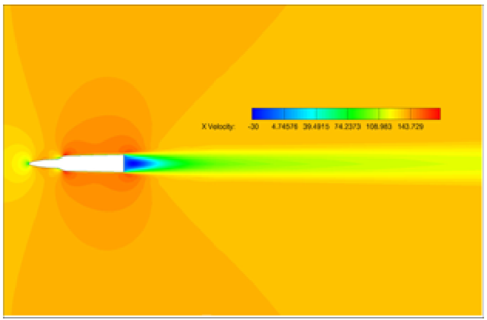

Figure 17. X-velocity of bullet shaped bluff body

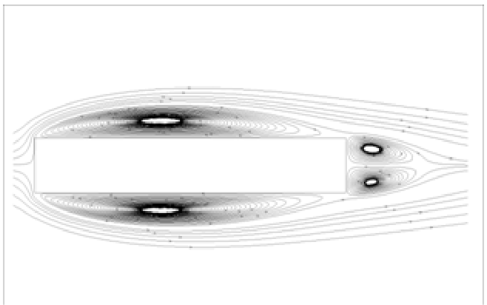

Figure 18. Eddy loop formation in rectangular bluff body

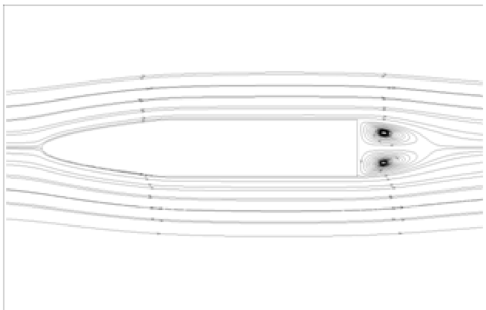

Figure 19. Eddy loop formation in radial rectangular bluff body

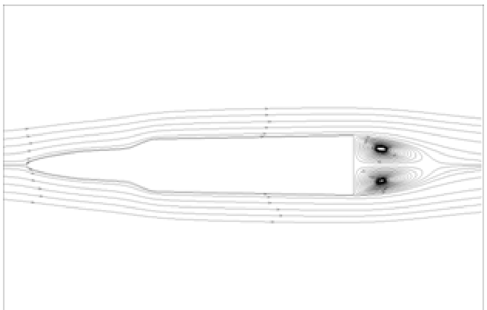

Figure 20. Eddy loop formation in bullet shaped bluff body

Fig 18, 19 and 20 shows the formation of the eddy loops around the bluff bodies. It was observed that the blunt area of the rectangular shape body assists the formation of eddy loops. Due to the discontinuity in the blunt shape, the streamlines flowing around the body were not smooth in nature and hence the generation of the eddy loops. On the other part, due to the smooth and continuous shape of the radial- rectangle and bullet shapes, there was no formation of the eddy loops near the sides i.e. walls of the body. Even if the formation of the loops at the end part of the radial-rectangle body was more than the bullet shape body, both compared to rectangular shape body were aerodynamic in nature.

Formation of eddy loops around the rectangular body was causing viscous flow which caused the drag to increase as the Mach number increases. The lift coefficient showed a peculiar pattern of decreasing with respect to increase in Mach number. The ideal graph of drag coefficient for aero foil shape was compared with the results to obtain the confirmation towards optimization. Generally, the drag coefficient peaks approximately till Mach 1.0 to 1.2 and begins to decrease again after the transition into the supersonic regime above approximately Mach 1.2. Thus, this shows from the computational data that the modifications in the rectangular bluff body till the bullet shape body were an optimizing stage of the bodyto make it as close as possible as an aerodynamic body. Table 3 shows the computed values of pressure force (P.F) and coefficient of drag (C_d) at different Mach numbers and the variation was noted. The drag value for rectangular, radial rectangular shape and bullet shape was optimized.*Fig 21 and 22* shows the variation of coefficient of drag and pressure forces of the bluff bodies with the variation of Mach number respectively. The pressure variation over the bluff body surface as the Mach number increases can be seen from the graph of P.F vs Mach number. It was found that as the Mach number increases, in a bluff body, coefficient of drag increases after comparing it to simulation result.

Table 3. Computational Output

Sr. No.	Bluff Body	Mach No.					
		0.4		0.8		1.5	
		P. F	**C_d**	**P. F**	**C_d**	**P. F**	**C_d**
1.	Rectangle	1472	0.1289	5891.4	0.1293	20701	0.464
2.	Radial Rectangle	515.2	0.0511	2083	0.0509	7402	0.178
3.	Bullet shaped	557.2	0.0054	2022	0.00215	7016	0.0537

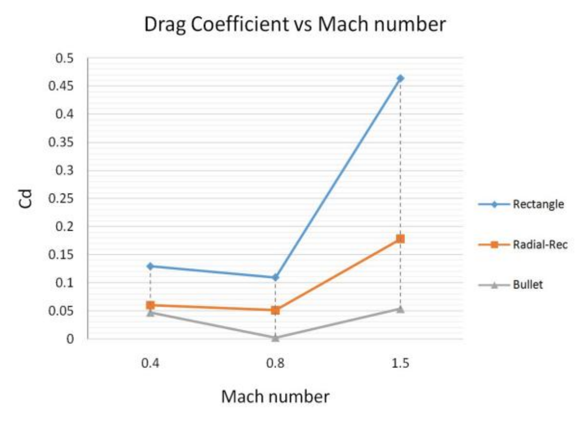

Figure 21. Drag coefficient vs Mach number

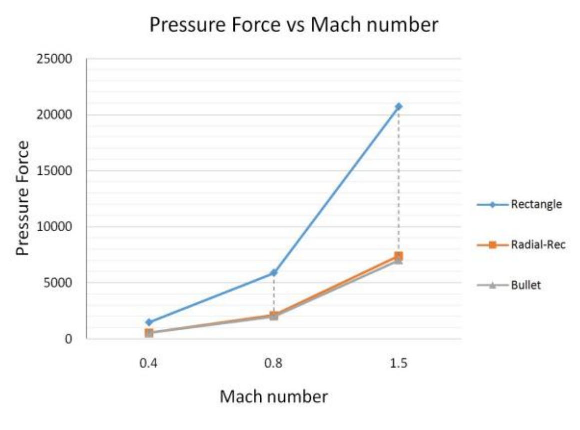

Figure 22. Pressure Force vs Mach number

VII. CONCLUSION

In above section, three test cases of bluff bodies; mainly two-dimensional rectangular body, radial rectangular shape and bullet shaped body were optimised. Further, the CFD results were obtained using commercial software ANSYS- Fluent. The aerodynamic coefficients and physics behind bluff bodies were studied and analysed. It is concluded that bullet shaped body is close to aerofoil shape and is aerodynamically best among all the cases.

REFERENCES

[1]. 'Bluff-body Aerodynamics', Guido Buresti, International Advanced School on Wind-Excited and Aeroelastic Vibrations of Stuctures, Genoa, June 12-16, 2000

[2]. 'Numerical simulationand visualization of flow around rectangular bluff bodies', Xuyong Ying et al., The Seventh International Colloquium on Bluff Body Aerodynamics and Applications (BBAA7) Shanghai, China, September 2-6, 2012

[3]. 'Computationa Study of Flow around a Simplified 2D Ahmed Body', Deepak Kumar Kalyan et al., International Journal of Engineering Science and Innovative Technology (IJESIT) Volume 2, Issue 3, May 2013

[4]. 'Stability Properties of 2D Flow around Ahmed Body', W. Stankiewicz et al., Mathematical Modeling and Analysis 2005, Proceedings of the 10th International Conference MMA2005 & CMAM, Trakai 2005 Technika, ISBN 9986-05-924-0

[5]. 'CFD analysis of 2D unsteady flow around a square cylinder', Gera. B et al., International Journal Apllied Engineering Research, Dindigul, Volume 1, No. 3, 2010

[6]. 'Aerodynamic Analysis of Ahmed Body', Rehan Salahuddin Khan et al., International Journal of Engineering Trends and Technology (IJETT), Volume 18 No. 7, Dec-2014

[7]. 'CFD Analysis of Different Bluff Bodies', Sibha Veerendra Singh et al., International Journal of Novel Research in Electrical and Mechanical Engineering, Volume-2, Issue-3, Sept-Dec 2015

[8]. 'Methods for the Drag Reduction of Bluff Bodies and their Application to Heavy Road- Vehicles', G. Buresti et al., 1st Interim Report Contract between CRF and DIA, DDIA 2007-6, October 2007

[9]. 'Bluff Body Aerodynamics and Wake Control', Efstathios Konstantinidis et al., Department of Mechanical Engineering, University of Wastern Macedonia, Bakola & Sialvera, Kozani-50100, Greece

[10]. 'Numerical Investigation of the Flow around a Rectangular Cylinder near a Solid Wall', Stafano Malavasi et al., BBAA VI International Colloquium on Bluff Bodies Aerodynamics & Applications, Milano, Italy, July, 20-24 2008

[11]. 'Application and Analysis of RANS based Turbulence Models for Bluff Body Aerodynamics', Sanket A. Unhale, Mechanical Engineering, Texas Tech University, Dec. 2004

[12]. 'PDF modelling of a Bluff-body stabilized turbulent flame', M. Muradoglu et al., Combustion and Flame (elsevier), 11 July 2002

[13]. 'Turbulence Model and Boundary Conditions for Bluff Body Flow', M. E. Young et al., 15th Australasian Fluid Mechanics Conference, The University of Sydney, Australia, Dec 2004